August 27-31, 2023
FLORENCE - ITALY
16th International Conference on Wind Engineering
ICWE 16

VIV modes competition of long-span bridges with closely-spaced multi-modes

Wei Cui, Lin Zhao, Yaojun Ge

Department of Bridge Engineering, Tongji University, Shanghai, China, cuiwei@tongji.edu.cn, zhaolin@tongji.edu.cn, yaojunge@tongji.edu.cn

SUMMARY:
For the flexible long-span bridge, the VIV lock-in regions for multiple closely-spaced multi-modes are overlapped. However, field observation of VIV events shows that normally only one mode can be excited about certain wind speeds. This paper proposes analytical formulas to examine the evolution of the multi-mode amplitude, and results show that mode competition determines the excited mode during VIV events of long-span bridges.

Keywords: vortex-induced vibration; nonlinear dynamics; modes competition

1. GENERAL INSTRUCTIONS

Vortex-induced vibration (VIV) is a major concern for long-span bridge decks, which may happen especially for long-span bridges. Traditionally, VIV events is observed as long as the wind speed falls within the lock-in region. However, VIV phenomena is normally analyzed at single modes without the consideration of multi-modes coupling(Ehsan and Scanlan, 1990). Because of the flexibility of long-span bridges, the dynamics modes frequencies are closely-spaced, the VIV lock-in regions for nearby modes are possibly overlapped, such as shown in Figure 1. The field observation of bridge on which VIV events happened shows that only one mode was excited while the the VIV lock-in region of other mode also covered the wind speeds during VIV events (Zhao et al., 2022). This study proposes an analytical framework to study the VIV amplitudes evolution between two nearby modes, and it shows that mode competition determines the excited mode for long-span bridge during VIV events.

2. THEORETICAL ANALYSIS OF VORTEX-INDUCED VIBRATION OF FLEXIBLE BRIDGE

At the arbitrary location x along the bridge deck with span as L, the governing motion equation for nonlinear vortex-induced vibration is

$$M(x)\frac{d^2z(x)}{dt^2}+C(x)\frac{dz(x)}{dt}+K(x)z(x)=\rho U^2D\left[Y_1\left[1-h\left(\frac{z(x)}{D}\right)\right]\frac{\frac{dz(x)}{dt}}{U}+Y_2\frac{z(x)}{D}\right] \tag{1}$$

where $z(x)$ is the vibration amplitude of bridge deck at location x, M-C-K are the structural mass, damping and stiffness, respectively.

If at certain wind speeds, there are two potential modes excited by vortex-induced effect, the vibration can be considered as the superposition of two modes (double degrees of freedom, DDOF). The situation that VIV lock-in region more than two modes contain the same wind speed is extreme rare, which will not be considered. The structural motion along span can be considered as:

$$z(x) = \phi_1(x)y_1 + \phi_2(x)y_2 = \begin{bmatrix}\phi_1(x) & \phi_2(x)\end{bmatrix}\begin{bmatrix}y_1\\ y_2\end{bmatrix} \tag{2}$$

Then the governing equation becomes as

$$\begin{bmatrix}m_1 & \\ & m_2\end{bmatrix}\begin{bmatrix}\frac{d^2y_1}{dt^2}\\ \frac{d^2y_2}{dt^2}\end{bmatrix} + \begin{bmatrix}2m_1\omega_1\xi_1 & \\ & 2m_2\omega_2\xi_2\end{bmatrix}\begin{bmatrix}\frac{dy_1}{dt}\\ \frac{dy_2}{dt}\end{bmatrix} + \begin{bmatrix}m_1\omega_1^2 & \\ & m_2\omega_2^2\end{bmatrix}\begin{bmatrix}y_1\\ y_2\end{bmatrix} = \\ \boldsymbol{\phi}^2\rho U^2DL\boldsymbol{Y}_1\begin{bmatrix}\frac{dy_1}{dt}\\ \frac{dy_2}{dt}\end{bmatrix}/U + \boldsymbol{\phi}^2\rho U^2DL\boldsymbol{Y}_2\begin{bmatrix}y_1\\ y_2\end{bmatrix}/D - \boldsymbol{\phi}^2\rho U^2DL\boldsymbol{Y}_1\boldsymbol{h}\left(\frac{\phi_1(x)y_1+\phi_2(x)y_2}{D}\right)\begin{bmatrix}\frac{dy_1}{dt}\\ \frac{dy_2}{dt}\end{bmatrix}/U \tag{3}$$

in which

$$\boldsymbol{\phi}^2 = \int_0^1 \begin{bmatrix}\phi_1(x/L)\\ \phi_2(x/L)\end{bmatrix}\begin{bmatrix}\phi_1(x/L) & \phi_2(x/L)\end{bmatrix}dx = \begin{bmatrix}\phi_{11} & 0\\ 0 & \phi_{22}\end{bmatrix}$$

and $\phi_{12} = 0$ because of modal shape orthogonality, m_1, ξ_1, ω_1 are modal mass, damping coefficient and frequency for first mode and m_2, ξ_2, ω_2 are similar quantities for second mode. For the nonlinear aeroelastic function, the modal shape integral will be included into $\boldsymbol{h}()$, which will be explicitly discussed later. $\boldsymbol{Y}_1, \boldsymbol{Y}_2$ are linear aeroelastic damping, linear aeroelastic stiffness depending on the vibration frequency ω_1 and ω_2 of corresponding mode. $\boldsymbol{h}()$ is nonlinear aeroelastic damping function $\boldsymbol{h}() = \text{diag}\begin{bmatrix}h_1() & h_2()\end{bmatrix}$.

Next, the non-dimensional motion is defined as $\eta = y/D$, K is the reduced frequency $K = \omega\frac{D}{U}$, and $\dot{\eta}$ indicate differentiation of η with respect to the dimensionless time $\tau = U\frac{t}{D}$. The governing equation in dimensionless form is

$$\begin{bmatrix}\ddot{\eta}_1\\ \ddot{\eta}_2\end{bmatrix} + \begin{bmatrix}2K_1\xi_1 & \\ & 2K_2\xi_2\end{bmatrix}\begin{bmatrix}\dot{\eta}_1\\ \dot{\eta}_2\end{bmatrix} + \begin{bmatrix}K_1^2 & \\ & K_2^2\end{bmatrix}\begin{bmatrix}\eta_1\\ \eta_2\end{bmatrix} = \boldsymbol{\phi}^2\boldsymbol{m}^*\boldsymbol{Y}_1\begin{bmatrix}\dot{\eta}_1\\ \dot{\eta}_2\end{bmatrix} - \boldsymbol{m}^*\boldsymbol{Y}_1\boldsymbol{h}(\eta_1,\eta_2)\begin{bmatrix}\dot{\eta}_1\\ \dot{\eta}_2\end{bmatrix} + \boldsymbol{\phi}^2\boldsymbol{m}^*\boldsymbol{Y}_2\begin{bmatrix}\eta_1\\ \eta_2\end{bmatrix} \tag{4}$$

where $\boldsymbol{m}^*$ is the mass ratio matrix $\boldsymbol{m}^* = \rho D^2L\begin{bmatrix}m_1 & \\ & m_2\end{bmatrix}^{-1}$.

The above equation can be rewritten in compact matrix format,

$$\ddot{\boldsymbol{\eta}} + [\boldsymbol{\varepsilon} + \boldsymbol{g}(\boldsymbol{\eta})]\dot{\boldsymbol{\eta}} + \boldsymbol{\kappa}^2\boldsymbol{\eta} = 0 \tag{5}$$

where $\boldsymbol{\eta} = \begin{bmatrix}\eta_1\\ \eta_2\end{bmatrix}$, $\boldsymbol{\varepsilon} = \begin{bmatrix}2K_1\xi_1 & \\ & 2K_2\xi_2\end{bmatrix} - \boldsymbol{\phi}^2\boldsymbol{m}^*\boldsymbol{Y}_1$, $\boldsymbol{\kappa}^2 = \begin{bmatrix}K_1^2 & \\ & K_2^2\end{bmatrix} - \boldsymbol{\phi}^2\boldsymbol{m}^*\boldsymbol{Y}_2$ and
$\boldsymbol{g}(\boldsymbol{\eta}) = \boldsymbol{m}^*\boldsymbol{Y}_1\boldsymbol{h}(\eta_1,\eta_2)$

Supposing the solutions to Eq. (5) are harmonic with small perturbation as:

$$\eta_1 = A_1 \cos(\kappa_1 \tau + \psi_1) + o(\varepsilon_1) \quad \eta_2 = A_2 \cos(\kappa_2 \tau + \psi_2) + o(\varepsilon_2) \tag{6}$$

Then the coupled amplitudes evolutionary function is

$$\dot{A}_1 = -A_1 \sin^2(\kappa_1 \tau + \psi_1)[\varepsilon_1 + g_1(\eta_1, \eta_2)] \quad \dot{A}_2 = -A_2 \sin^2(\kappa_2 \tau + \psi_2)[\varepsilon_2 + g_2(\eta_1, \eta_2)] \tag{7}$$

3. VIV PARAMETERS DETERMINATION FROM SECTIONAL MODEL TESTS

Since it it difficult to directly evaluate the VIV aeroelastic parameters on full-scale bridge, the sectional model tests were conducted to examine the VIV response and determine the aeroelastic parameters including Y_1, Y_2 and nonlinear aeroelastic force function $h()$. If the nonlinear aeroelastic force is expanded into Taylor series as:

$$g_1(\eta) = \sum_{i=1}^{N} b_i \eta^i \quad h(\eta) = \sum_{i=1}^{N} a_i \eta^i \tag{8}$$

where $b_i = a_i m_1 Y_1$. Next, the amplitude evolution function became as

$$\dot{A}_1 = -A_1 \sin^2(\kappa_1 \tau + \phi_1)\left[\varepsilon_1 + g_1(\eta)\right] = A_1 \sin^2(\kappa_1 \tau + \phi_1)\left[\varepsilon_1 + \sum_{i=1}^{N} b_i A_1^i \cos^i(\kappa_1 \tau + \phi_1)\right] \tag{9}$$

Therefore, through averaging theory, the amplitude evolution during one cycle is

$$\dot{A}_1 = -A_1 \left[\varepsilon_1 I_0 + \sum_{i=1}^{N/2} b_{2i} I_{2i} A_1^{2i}\right] \tag{10}$$

where $I_0 = \frac{1}{2\pi}\int_{-\pi}^{\pi} \sin^2(T+\phi)dT = \frac{1}{2}$ and $I_{2i} = \frac{1}{2\pi}\int_{-\pi}^{\pi} \sin^2(T+\phi)\cos^{2i}(T+\phi)dT = \frac{2i-1}{2i+2} I_{2i-2}$. Figure 2 plots the amplitude evolution rate for $K = 0.7313$ ($U = 8$ m/s for mode 1), of which the aeroelastic parameters were determined through sectional model tests in wind tunnel.

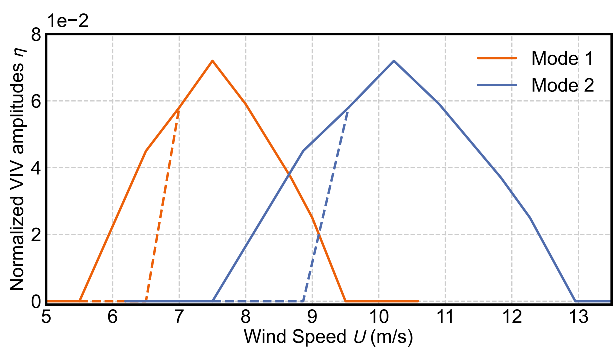

Figure 1. The VIV lock-in region for two modes

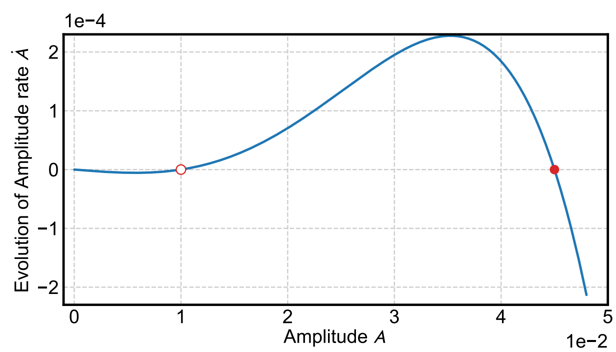

Figure 2. amplitude evolutionary rate for $K = 0.7313$

4. MODE COMPETITION OF COUPLED VIV BETWEEN TWO MODES

For the VIV dynamics system with two modes, the aeroelastic parameters are depending on the reduced frequency. The coupled amplitudes evolution formula is derived as:

$$\dot{A}_1 = -A_1 \left\{ \varepsilon_1(\kappa_1) I_0 + \sum_{i=1}^{N/2} a_{2i}(\kappa_1) I_{2i} \sum_{j=0}^{i} \binom{2i}{2j} \phi_1^{2j+2} \otimes \phi_2^{2i-2j} A_1^{2j} A_2^{2i-2j} \right\} \tag{11a}$$

$$\dot{A}_2 = -A_2 \left\{ \varepsilon_2(\kappa_2) I_0 + \sum_{i=1}^{N/2} a_{2i}(\kappa_2) I_{2i} \sum_{j=0}^{i} \binom{2i}{2j} \phi_1^{2j} \otimes \phi_2^{2i-2j+2} A_1^{2j} A_2^{2i-2j} \right\} \tag{11b}$$

where $\phi_1^j \otimes \phi_2^i = \int_0^1 [\phi_1(x/L)]^j [\phi_2(x/L)]^i dx$

Based on the aeroelastic parameters determined through wind tunnel tests, the coupled 2-directional amplitudes evolutionary function are plotted in Figure 3. For both $U = 8$ m/s and $U = 9$ m/s, there are only one stable equilibrium point, and other equilibrium points are either unstable or saddle point. Mode competition dominates the excited mode during VIV events.

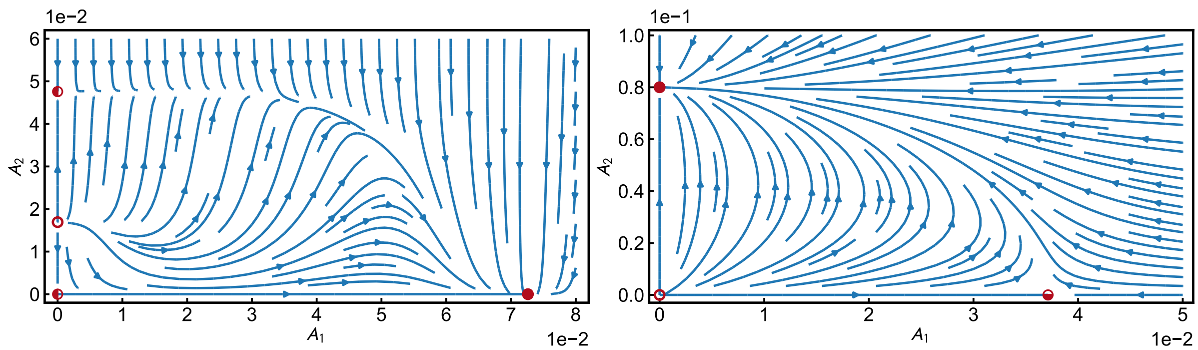

(a) $U = 8$ m/s

(b) $U = 9$ m/s

Figure 3. Phase plane portrait of VIV Mode competition at different wind speeds

5. CONCLUSIONS

This paper proposes a coupled multiple modes formula to calculate the VIV amplitudes evolution. The aeroelastic parameters during VIV lock-in region were determined through sectional model in wind tunnel tests, and then coupled amplitudes evolution can be determined by the formula proposed in this study.

ACKNOWLEDGEMENTS

The authors gratefully acknowledge the support of National Key Research and Development Program of China (2021YFF0502200) and National Natural Science Foundation of China (52008314).

REFERENCES

Ehsan, F. and Scanlan, R. H., 1990. Vortex-induced vibrations of flexible bridges. Journal of Engineering Mechanics 116, 1392–1411.

Zhao, L., Cui, W., Shen, X., Xu, S., Ding, Y., and Ge, Y., 2022. A fast on-site measure-analyze-suppress response to control vortex-induced-vibration of a long-span bridge. Structures 35, 192–201.